Spring 2016

Up-converted Emissions of Er3+ Doped Gd2(WO4)3 Phosphors

Grayson L. Wiggins

UP-CONVERTED EMISSIONS OF Er^{3+} DOPED $Gd_2(WO_4)_3$ PHOSPHORS

by

GRAYSON L. WIGGINS

(Under the Direction of Xiao-Jun Wang)

ABSTRACT

In this work, the up-conversion (UC) emissions of Er^{3+} in a gadolinium tungstate host was investigated to analyze the possible processes of up-conversion by 1500 nm and 980 nm excitation. Studies were conducted to see how the $^4S_{3/2} \rightarrow {}^4I_{15/2}$ transition changed with varying current through the excitation source, varying excitation wavelength, and doping concentration. Power dependent studies revealed that under 1500 nm excitation the $^4S_{3/2} \rightarrow {}^4I_{15/2}$ transition needed 3 photons, while 980 nm excitation could do the same transition with 2 photons. It was found that 1500 nm could produce more efficient red emission due to the $^4I_{9/2} \rightarrow {}^4I_{15/2}$ transition only needing 2 photons. Concentration dependence studies revealed many trends of how up-conversion processes varied with erbium ion separation. The number of photons used to UC 980 nm decreases as concentration increases, meaning that the mechanism depends on energy transfer UC and the inefficiency of green emissions at higher concentration is due to concentration quenching. UC of 1500 nm also uses less photons as concentration increases; red and green emissions are not as dependent on energy transfer UC as 980 nm UC. Also, as concentration increases past the point least photon use, the erbium ions start cross relaxing causing the number of photons used to increase rapidly. It was found that even after cross relaxation becomes the dominant UC process, the intensity still increases as concentration increases until a point where quenching starts to take effect.

INDEX WORDS: Gadolinium tungstate, trivalent erbium, up-conversion, luminescence

UP-CONVERTED EMISSIONS OF Er^{3+} DOPED $Gd_2(WO_4)_3$ PHOSPHORS

by

GRAYSON L. WIGGINS

B.S., Georgia Southern University, 2013

A Thesis Submitted to the Graduate Faculty of Georgia Southern University in Partial Fulfillment of the Requirements for the Degree

MASTER OF SCIENCE

STATESBORO, GEORGIA

UP-CONVERTED EMISSIONS OF Er^{3+} DOPED $Gd_2(WO_4)_3$ PHOSPHORS

by

GRAYSON L. WIGGINS

Major Professor:	Xiao-Jun Wang
Committee:	Li Ma
	Marshall Ming

Electronic Version Approved:
May 2016

TABLE OF CONTENTS

Page

ACKNOWLEDGMENTS

This thesis could not have been completed without the help of Dr. Wang. He provided the knowledge, expertise, and focus throughout the length of this work. Also, Dr. Ma was invaluable in demonstrating how equipment should be used, and how they should be fixed if problems arise. I would like to thank both of them for their constant support and for the opportunity they gave me.

I would also like to thank Dr. Feng Liu, at the University of Georgia, for performing the XRD experiments on the samples used in this thesis. His experiments were integral in proving that the data came from reliable samples.

Lastly, I would like to thank the faculty and staff, as well as the students, of the Georgia Southern University Physics Department. They always provide strong advice and valuable research sources with which to work. The students were very courteous to keep lab areas sanitary for my synthesis procedures.

LIST OF TABLES

Page

LIST OF FIGURES

Page

CHAPTER 1

INTRODUCTION

Luminescence

This work focuses on studying the processes and mechanisms of a photoluminescent phenomenon called photon up-conversion, or multi-photon excitation. Photoluminescence is the emission of light as a result of absorption of photons, and is a type of luminescence. Luminescence is the emission of light by a substance not resulting from heat and was first introduced by Eilhard Wiedermann in 1888 to describe materials that were either phosphorescent or fluorescent [1]. After this term was published, the scientific community found a wide range of different mechanisms for luminescence; chemiluminescence, electroluminescence, and mechanoluminescence [2]. G. G. Stokes introduced the term fluorescence in 1852 [3], and for years afterwards, the distinction between fluorescence and phosphorescence was not well defined. The difference was based on the duration of emission after the end of excitation; fluorescent emissions took tens of nanoseconds, and phosphorescent emissions lasted over a millisecond. However, such stipulation is insufficient because there are long-lived fluorescent emissions and short-lived phosphorescent emissions whose durations are extremely close, taking only hundreds of nanoseconds to relax. In 1929, Francis Perrin stated that the usual condition for observing phosphorescence is that the excited species passes through an intermediate state before emission [4]. In more precise terms, the spin multiplicity is retained for fluorescence, whereas phosphorescence involves a change in spin multiplicity. Another difference is that fluorescence is typically a localized phenomenon while phosphorescence is a mobilized luminescence process.

Materials that are either phosphorescent or fluorescent are known as phosphors. Phosphors are mainly solid inorganic crystals, ceramics, or glasses that consist of a host lattice with intentionally doped impurities as activators. Incident light is either absorbed via the host lattice or the impurities, but the emission almost always originates from the impurities, also known as luminescence centers. This signifies that the host material only needs to have minimal effect on the luminescence centers, unless transferring energy to the impurities. Therefore, the host needs to be chemically and thermally stable, have low phonon energy, and wide band gaps allows the emissions from the dopants out without absorption.

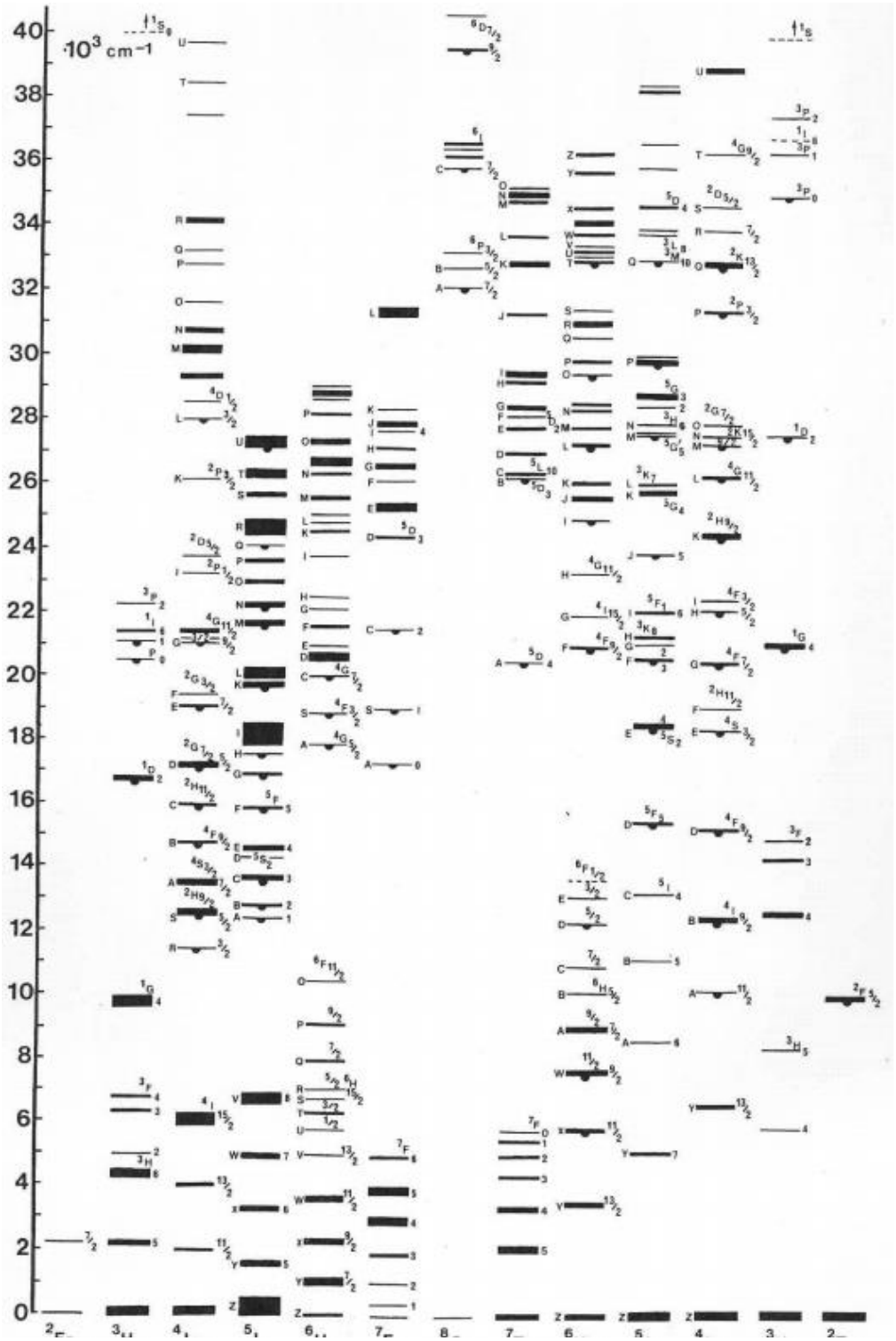

Fig 1.1: Dieke diagram showing the energy levels of the trivalent rare-earth ions in the host crystal $LaCl_3$, compiled by Dieke in 1963 [18].

Energy Levels

Figure 1.1 is a diagram of the electronic energy levels of trivalent lanthanide ions, complied by Dieke and Crosswhite in 1963. These electronic states are typically denoted by style presented by Russell and Saunders: $^{2S+1}L_J$, where L is the angular orbital momentum of the state, S is the spin momentum, and J is the total angular momentum. In an atom, the electrons travel on these energy states, by absorbing or emitting photons. Absorbing photons causes the electrons to excite to a higher energy level, while emitting photons causes the electrons to relax to a lower energy level. There are many interesting phenomenon going on inside the electron orbitals, but this work is mainly concerned with down- and up-conversion processes.

Down-Conversion & Up-Conversion

The most general photoluminescence process is down-conversion and happens in nearly all phosphors. The phosphor absorbs a high energy photon, blue or UV, and moves to an excited state, then, as it decays back to the ground state it emits one or multiple photons of low energy. In the case of erbium, a doped phosphor can absorb a blue photon and emit green, red, and even infrared photons. It was theorized by N. Bloembergen [5], that this process could be reversed by using infrared photons to emit blue photons. Indeed, this process was first observed by F. Auzel in 1966 and was named up-conversion [6]. However, due to the lower energy of the excitation photons, the host material needs to have low phonon energies in order to keep the impurities from emitting non-radiative vibrational energy instead of light. More detail will be put into the mechanics of up-conversion in the next chapter.

Host Crystals & Dopants

Among different compounds including aluminates, silicates, and borates, phosphors utilizing tungstate hosts are very popular because of their high thermal and chemical stability to powerful irradiation [7]. Tungstate lattices are also excellent host materials for lanthanide ions [8, 9]. $MgWO_4$, $CaWO_4$, $SrWO_4$, and $CdWO_4$ have been thoroughly studied for more than 50 years because of their great technological importance [10]. In order for the tungstate to successfully host trivalent lanthanide ions, it needs to be bonded with another trivalent metal. One great candidate is gadolinium, it is a poor absorber of visible and infrared radiation and has an atomic size that is comparable to the other lanthanide ions. In addition to causing few

distortions to the crystal structure, gadolinium tungstate offers low phonon energy, high photochemical stability, and high quantum yield [11].

The introduction of trivalent rare-earth ions, especially lanthanides (Ln^{3+}), in host matrices as luminescent centers has been an improvement in the field of luminescent materials [12]. Lanthanide ions show interesting fluorescence properties due to the optical transitions within the $4f^n$-electronic manifold. The f-electrons are well shielded from the chemical environment and therefore, almost retain their atomic characteristics. Usually, when light is absorbed by matter, only a small amount get reflected back because the rest is converted into vibrational energy due to the chemical bonds. However, the rare-earth ions are bound by electrons that do not absorb visible light. Consequentially, the f-f emission spectra consist of sharp narrow lines, which creates the possibility of using Ln^{3+} ions as effective and efficient luminescent centers.

Applications

In this work, the lanthanide being investigated is trivalent erbium, Er^{3+}, since it's one of the most popular and efficient ions for obtaining near-infrared to visible up-conversion. Erbium's ability to up-convert 1500 nm infrared emission which is useful for optical amplification in fiber optics [13] and lasers [14]. Optical up-conversion is very popular in many technologically advanced fields. Such fields include infrared indicator cards, bio-labels [15], three-dimensional displays [16], and photovoltaics [17, 18]. For photovoltaics, silicon solar cells cannot utilize infrared photons, so the use of an erbium phosphor can convert 'ignored' photons into usable visible photons, increasing the energy efficiency. The prospect of this thesis is to analyze the up-conversion process of 1500 nm light by trivalent erbium doped gadolinium tungstate ($Gd_2(WO_4)_3:Er^{3+}$) including visible and near infrared spectra, X-ray diffraction characterization, and incident power dependence.

Summary

In the next chapter, the various up-conversion processes are introduced and described using rate equations. Figures are used to display how the photon number of a transition can be used to visualize the different UC mechanisms. Lastly, there is a description of phonon energies and a definition of multi-photon excitation and multi-phonon relaxation.

In chapter three, the stoichiometric calculations are carried out in order to illustrate the acuity of the synthesis process. Then, a description of the co-precipitation synthesis process is presented. Chapter four contains the equipment used in this thesis and a description of the experimental spectroscopic setup is given. Also, included is the mathematical transforms that were applied to the experimental data during analysis.

In chapter five is the complete resulting works of this thesis. X-ray diffractograms are presented to state the purity of the synthesized samples. Concentration curves are also included, describing how dependent the intensity is on the distance between ions. Power dependent curves are shown to illustrate how the double-logarithmic slope changes with concentration. Photon number curves are then used to convey the slopes in terms of photons. Lastly, the photon numbers are used to discuss the possible mechanisms involved with the UC. In the last chapter, conclusions over the results of the data are discussed. The possible mechanisms involved and the most efficient up-conversion processes are identified.

References

[1] Wiedemann, Eilhard. "Uber Fluorescenz und Phosphrescenz, I. Abhandlung." *Annalen der Physik und Chemie.*Leipzig: Johann Ambrosius Barth, 1888, 446-69. Web.

[2] Valeur, Bernard, and Mário N. Berberan-Santos. "A Brief History of Fluorescence and Phosphorescence before the Emergence of Quantum Theory." *Journal of Chemical Education* 88.6 (2011): 731-38. Web.

[3] Stokes, G. G. "On the Change of Refrangibility of Light." *Philosophical Transactions of the Royal Society of London* 142.0 (1852): 463-563. Web.

[4] Perrin, Francis. *La Fluorescnence des Solutions, Induction Moléculaire, Polarisation et Durée D'émission, Photochemie*. Paris: Masson, 1929. Web.

[5] Bloembergen, N. "Solid State Infrared Quantum Counters." *Physical Review Letters* 2.3 (1959): 84-85. Web.

[6] Auzel, F. "Compteur quantique par transfert d'énergie entre deux ions de terres rares dans un tungstate mixte et dans un verre," *C.R. Acad. Sci. Paris* 262, 1016–1019 (1966).

[7] Mahlik, S. A. Lazarowska, B. Grobelna, and M. Gringberg. "Luminescence of Gd2(WO4)3:Ln3 at Ambient and High Hydrostatic Pressure." *Journal of Physics: Condensed Matter* 24.48 (2012): 485501. Web.

[8] Pang, M.I, J. Lin, and M. Yu. "Fabrication and Luminescent Properties of Rare Earths-doped Gd2(WO4)3 Thin Film Phosphors by Penchini Sol-gel Process." *Journal of Solid State Chemistry* 177.7 (2004): 2237-241. Web.

[9] Kodaira, Cláudia A., Hermi F. Brito, and Maria Cláudia F.c. Felinto. "Luminescence Investigation of Eu3 Ion in RE2(WO4)3 Matrix (RE=La and Gd) Produced Using the Pechini Method." *Journal of Solid State Chemistry* 171.1 (2003) 401-07. Web.

[10] Yen, W. M., Shigeo Shionoya, and Hajime Yamamoto. *Phosphor Handbook.* Boca Raton, FL: CRC/Taylor and Francis, 2007. Web.

[11] Sun, M. L. Ma, B.J. Chen, F. Stepongzi, F. Liu, Z.W. Pan, M.K. Lei, and X.J. Wang. "Comparison of Up-converted Emissions in Yb3, Er3 Co-doped Gd2(WO4)3 and Gd2WO6 Phosphors." *Journal of Luminescence* 152 (2014): 218-21. Print.

[12] Ronda, C. R., T. Justel, and H. Nikol. "Rare Earth Phosphors: Fundamentals and Applications." *Encyclopedia of Materials: Science and Technology* (2001): 8026-033. Web.

[13] Lisiecki, Radoslaw, Elzbieta Augustyn, Witold Ryba-Romanowski, and Michal Zelechower. "Er-doped and Er, Yb Co-doped Oxyfluoride Glasses and Glass-ceramics, Structural and Optical Properties." *Optical Materials* 33.11 (2011): 1630-637. Web.

[14] Grubb, S.G., K.W. Bennett, R.S. Cannon, and W.F. Humer. "CW Room-temperature Blue Upconversion Fibre Laser." *Electronics Letters* 28.13 (1992): 1243-44. Web.

[15] Niedbala, R., H. Feindt, K. Kardos, T. Vail, J. Burton, B. Bielska, S. Li, D. Milunic, P. Bourdelle, and R. Vallejo. "Detection of Analytes by Immunoassay Using Up-Converting Phosphors Technology." *Analytical Biochemistry* 293.1 (2001): 22-30. Web.

[16] Downing, E., L. Hesselink, J. Ralston, and R. MacFarlane. "A Three-Color, Solid-State, Three-Dimensional Display." *Science* 273.5279 (1996): 1185-189. Web.

[17] Strümpel, Claudia. "Application of Erbium-Doped Up-Converters to Silicon Solar Cells." Diss. Konstanz, Univ. 2007. Print.

[18] Stefan, Fischer. "Up-conversion of Sub-Band-Gap Photons for Silicon Solar Cells." Diss. Diss. Freiberg, Univ. 2010. Print.

CHAPTER 2

PRINCIPLES OF UP-CONVERSION

2.1 Introduction

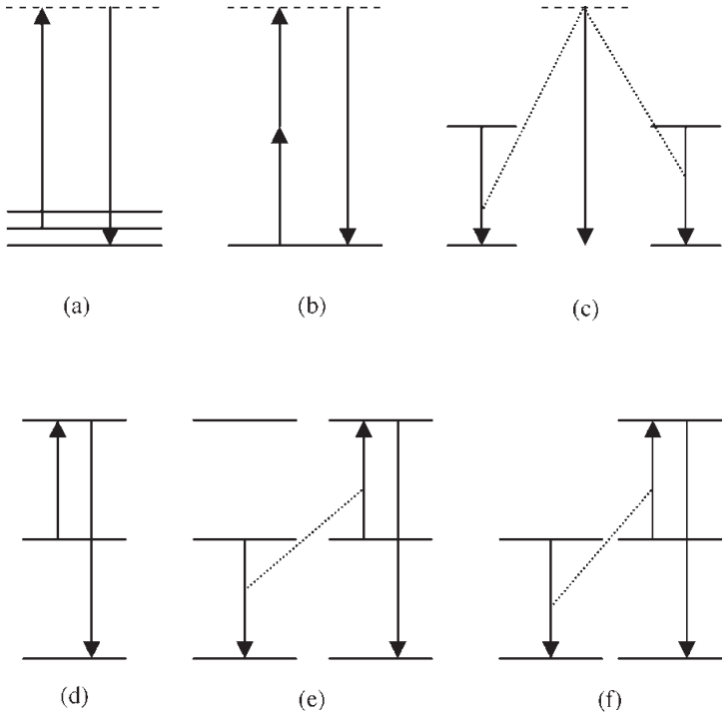

Fig. 2.1: Six of the most relevant processes that convert long-wavelength light into shorter-wavelength light. The processes include (a) anti-Stokes Raman emission, (b) second harmonic generation, (c) cooperative luminescence, (d) excited state absorption, (e) energy transfer up-conversion, and (f) sensitized energy transfer up-conversion. The dotted lines indicate non-radiative energy transfer processes, the dashed horizontal line indicate virtual states, and the arrows indicate excitation or emission transitions.

This chapter illustrates the mechanics of up-conversion (UC) processes in phosphors. Technically, up-conversion deals with absorbing photons of a certain energy E_1 and emitting photons with another energy E_2, such that $E_2 > E_1$. However, there exists many processes that result in the conversion of photons of a given wavelength into ones with shorter wavelengths. Figure 2.1 shows some examples of these processes, as well as, those considered to be up-conversion processes. These non-up-conversion processes include anti-Stokes Raman emissions (Fig. 2.1(a)), second harmonic generation (b), and cooperative luminescence (c). Figure 2.1(d-f) depicts the two-photon, or multi-photon, up-conversions processes that are relevant for the rest of this chapter. These processes are excited-state absorption (ESA), energy transfer up-

conversion (ETU), and sensitized energy transfer up-conversion, respectively [1]. The most important difference between up-conversion and the other processes in Fig. 2.1(a-c) is that UC depends on a real intermediate state, instead of one that is virtual [2]. This state must be able to store an excitation long enough to allow a second excitation photon to further excite the phosphor into the higher-lying excited state, typically at least a microsecond. Since UC relies on real energy levels only, very high excitation powers are not required in order to observe this effect. It is common for experimental data to show UC at excitation powers that are 5-10 orders of magnitude lower that those required for second harmonic generation [2]. This chapter will describe the photoluminescent processes integral to UC using rate equations, introducing band assignment, multi-photon excitation, and multi-phonon relaxation, as well as, deriving the erbium ion separation distance that will be used in Chapter 5.

2.2 GSA, ESA, ETU, and CR

The difference between sensitized energy transfer up-conversion and ETU is that in the former process the transfer is between two ions of different elements, whereas ETU is between two ions of the same element. Due to this distinction, sensitized energy transfer up-conversions will not be discussed further as this thesis is only concerned with erbium ions. For the remainder of this chapter, five main processes must first be described; ground state absorption (GSA), relaxation, ESA, ETU, and cross relaxation (CR), as depicted in Fig. 2.2, respectively.

2.2.1 Descriptions via Rate Equations

Fig. 2.2 also shows that UC processes must take place in a system containing at least three energy levels. Luminescent processes are generally described using rate equation, where the temporal change of the population density of the involved energy levels is formulated. The population density of the i-th energy level is defined to be N_i. GSA can cause changes in the population of the ground level, N_0. The change in the population is proportional to the population of the level and a term, G_{01}, describing the probability of this transition. Relaxations from higher energy levels can cause further changes to the ground level and their probabilities can be described using Einstein coefficients [3].

The probability of a transition within a free ion excited by incident radiation can be described by time-dependent perturbation theory [4]. The electric dipole transitions are of most

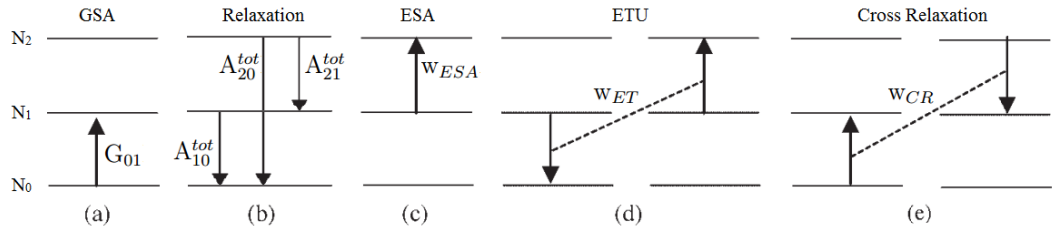

	GSA		relaxation		ESA	ETU	cross relaxation
$\dot{N}_0$ =	$-G_{01}N_0$	$+A_{10}^{tot}N_1$	$+A_{20}^{tot}N_2$			$+ w_{ET}N_1^2$	$- w_{CR}N_0N_1$
$\dot{N}_1$ =	$-G_{01}N_0$	$-A_{10}^{tot}N_1$		$+A_{21}^{tot}N_2$	$-w_{ESA}N_1$	$-2w_{ET}N_1^2$	$+2w_{CR}N_0N_2$
$\dot{N}_2$ =			$-A_{20}^{tot}N_2$	$-A_{21}^{tot}N_2$	$+w_{ESA}N_1$	$+ w_{ET}N_1^2$	$- w_{CR}N_0N_1$

Fig. 2.2: The five main processes of concern in the thesis, along with their rate equations. The processes are (a) ground state absorption, (b) relaxation, (c) excited state up-conversion, (d) energy transfer up-conversion, and (e) cross relaxation. Note the superscript *tot* on the A coefficient, this is defined as the sum of both radiative and non-radiative relaxation processes.

importance due to the fact that magnetic dipole transitions are orders of magnitude weaker. The probability of the electric dipole transition can be derived as:

$$G_{if} = \frac{\pi}{3n\epsilon_0 c_0 \hbar^2} I \left|\boldsymbol{\mu}_{if}\right|^2 \delta(\omega_0), \tag{2.1}$$

$$\boldsymbol{\mu}_{if} = \langle \psi_f | q\mathbf{r} | \psi_i \rangle, \tag{2.2}$$

where ω_0 is the angular frequency, $\boldsymbol{\mu}_{if}$ is the matrix element of the electric dipole moment, I is the intensity of the radiation, n is the refractive index of the absorbing medium, ε_0 is the permittivity in vacuum, c_0 is the speed of light in vacuum, and $\hbar$ is Planck's constant, h, divided by 2π. In the electric dipole moment (Eq 2.2), ψ_f and ψ_i are the wavefunctions of the final and initial states, respectively, and $\mathbf{r}$ is the position of the electron measured from the nucleus, and q is the elementary charge. The Dirac delta function $\delta(\omega_0)$ indicated the selectivity of the transition on the frequency of the incident light. To express realistic processes this function can be replaced with a line shape function $g(\omega)$. It can be seen from this that the transition probability is dependent on the intensity of the incident radiation, meaning that it is dependent on power.

When it comes to relaxation, the general form is:

$$\dot{N} = A^{tot}N = (A^{rad} + A^{nr})N, \tag{2.3}$$

where A^{tot} is the total rate of relaxation (decay rate). This includes A^{rad} radiative and A^{nr} non-radiative types of decay. These coefficients can be found experimentally by studying the decay rate of each energy level of interest. Non-radiative decay includes multi-phonon emission, as well as, all energy transfer mechanisms leading to the relaxation of the considered energy level without direct emission, such as CR.

Einstein developed a derivation for the probability of spontaneous radiative transition from initial state *i* to final state *f* on the basis of thermodynamic considerations [4]:

$$A_{if}^{rad} = \frac{1}{4\pi\epsilon_0}\frac{4n\omega_0^3}{3\hbar c_0^3(2J+1)}\left(\frac{n+2}{3}\right)^2\left|\boldsymbol{\mu}_{if}\right|^2, \tag{2.4}$$

where ω_0 is the mean angular frequency of the emission, (2J+1) is the degeneracy of the initial state and *n* is the refractive index of the surrounding medium. The $((n+2)/3)^2$ term is the local field correction for electric dipole transitions due to the influence of the surrounding crystal field [5].

The probability for an energy level to change population due to ESA, ETU or CR are denoted in terms or w_{ESA}, w_{ET}, and w_{CR}, respectively. The probability for ESA and ETU are derived in 2.3.3 to emphasize how dependent they are on the concentration.

2.3 Multi-photon Excitation

Since all UC processes depend on a real intermediate state [2], every time a low energy photon is absorbed by an erbium ion, it changes the population of two states. Therefore, if the number of excited states is known, then the number of photons can be counted. In order to appropriately introduce how to count the number of photons involved in an atomic transition, the concept of the band assignments must be introduced first. This reveals a better way to visualize what is going on in the ion. The basic procedure is to take an excitation spectra that down-converts high energy photons into multiple photons of the same lower energy.

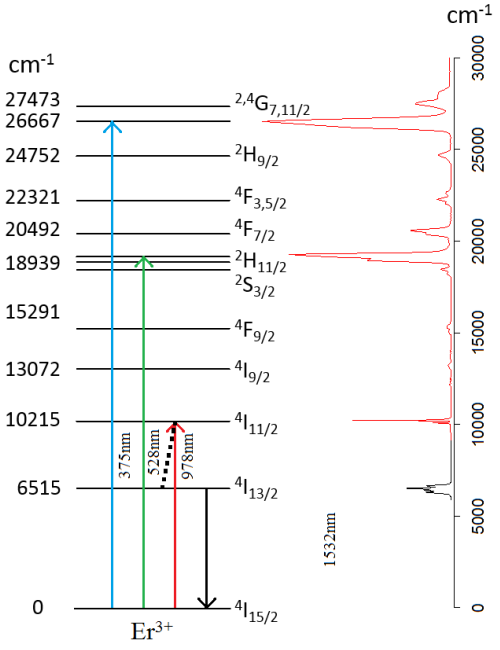

Fig 2.3: Excitation spectra monitoring the 1532 nm emissions, aligned with the energy levels of an erbium ion

2.3.1 Band Assignment

Figure 2.3 depicts an excitation spectra of one of the erbium doped gadolinium tungstate samples, excited from 300-1550 nm and monitored the emission of 1532 nm photons, on the right. The left side depicts how the high energy photons can shower down 1532 nm photons upon the energy levels. The intensity of the peaks on the right of Fig 2.3 correspond to how many 1500 nm photons are emitted: 375 nm makes 4 photons, 528 nm makes 3 photons, and 978 nm & 1500 nm makes 1 photon.

The peaks also point to the energy band to which they are assigned. 375 nm is a GSA to the $^4G_{11/2}$ energy level. 528 nm corresponds to the $^2H_{11/2}$ level, 978 nm is the $^4I_{11/2}$, and 1500 nm relies on the $^4I_{13/2}$ energy level.

2.3.2 1500 nm & 980 nm Up-Conversion

Fig. 2.2(a) and (c) show what happens when the ion is excited form is ground state, or from an excited state, respectively. The probability of the GSA/ESA up-conversion process is a product of the probability of stimulated absorption:

$$G_{01} \approx w_{ESA}, \tag{2.5}$$

$$w_{GSA/ESA} = G_{01} w_{ESA} \approx G_{01}^2, \tag{2.6}$$

Since both processes are stimulated absorption, the probability can be approximately equal. This process takes place within a single ion without including energy transfer [3].

In contrast, energy transfer processes are more complex. When two ions are in an excited state, this is when energy transfer up-conversion can take place, as shown in Fig. 2.2(d). Due to this process, one of the ions de-excite to a lower energy level, while the second ion is further excited to a higher-energy level. By assigning the transfer probability from one ion to the other, it can be shown that the probability of the excitation of the highest energy level of the acceptor ion is:

$$w_{GSA/ETU} = G_{01}^2 w_{ET}^2 N_0^2, \tag{2.7}$$

This shows that ETU depends quadratically on the density of ions in their ground state, N_0, which is a measure of the doping concentration. Note that GSA/ESA is independent of N_0, but

this should not be confused with $\dot{N}=G_{01}N$, which depends linearly on doping concentration [3]. The effects of concentration quenching are discussed in Section 2.5.

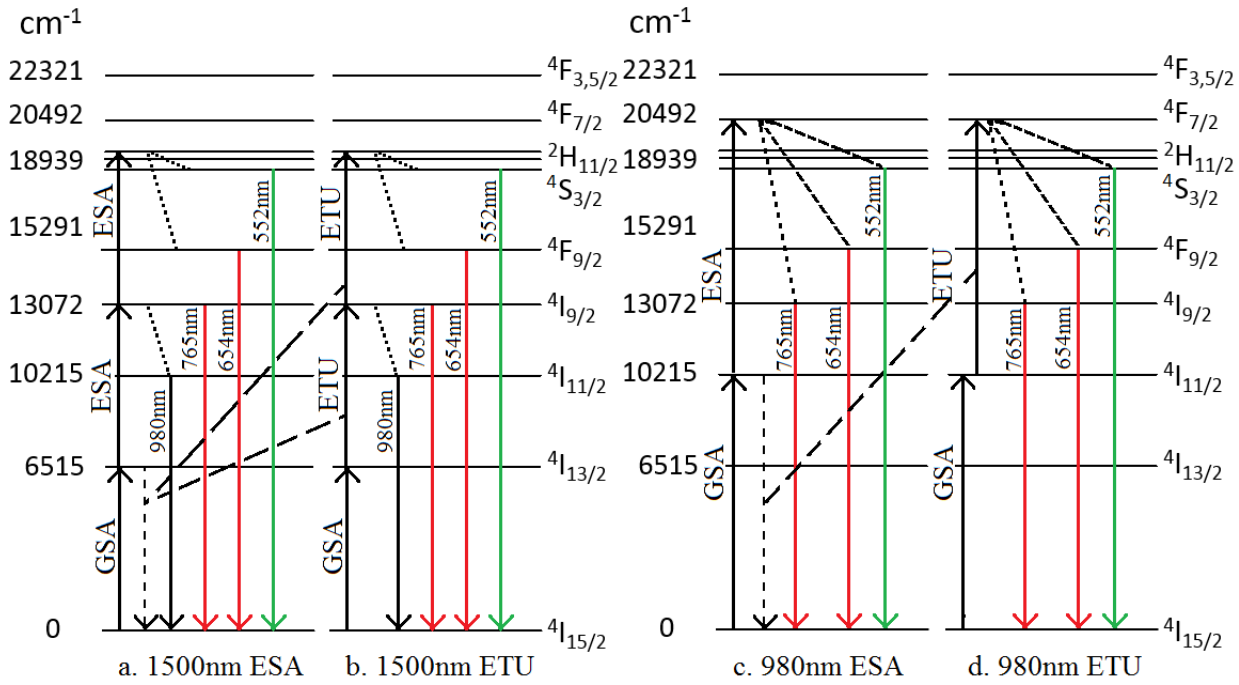

Fig 2.4(a, b, c, d): Up-conversion schematics of possible processes. GSA, ESA, and ETU processes are labelled for both 1500 nm and 980 nm UC. The dotted lined indicate non-radiative processes. In (d) there is only one chance for UC via ETU, while in (b) there are 2 possibilities for this transfer.

When the down-conversion process from Fig 2.4 is reversed, it becomes Figure 2.4. The Fig 2.4 depicts the ways that GSA, ESA, and ETU can give rise to the different emitted types of light. Every process is dependent on the initial GSA, this populated excited state can then either up-convert via ESA or ETU. Simply, the erbium ions need to be close enough to transfer their energies. Inversely, if the ions are too close then they would rather transfer the energy than up-convert it, via CR. Fig 2.4 states that there are more places for ETU to take place in 1500 nm UC than in 980 nm UC. This means that there also more places for cross relaxation to occur also.

2.4 Power Dependence

In order to measure the power dependence of the up-conversion processes, all of the samples' spectra were taken with varying current passing through the excitation source. When the current changed, for instance increased, the power (P) of the light leaving the excitation was proportionally increased. The intensity of the emission (I) is proportional to the power raised to a whole integer n (Eq 2.8). Taking the log of the two quantities makes the n a scalar rather than a power (Eq 2.9). Mathematically, n is the slope of the data in the double-logarithmic plot of power versus intensity (Eq 2.10). Physically, n is the number of photons up-converted to produce one higher energy photon. These concepts are used in Section 5.3.

$$I \propto P^n, \tag{2.8}$$

$$\log(I) \propto n\log(P), \tag{2.9}$$

$$\text{slope} = n = \frac{\log(I)}{\log(P)} = \text{number of photons absorbed to carry out transition} \tag{2.10}$$

2.5 Concentration Quenching

Fig. 2.2(e), cross-relaxation, is the fifth process depicted and as stated before, it is the opposite of ETU: one ion is excited to a higher energy state and the other is de-excited. The distinction between ETU and cross-relaxation is the highest excited state: if, after the process, none of the ions is in a higher energy state than either of the ions was before the process, this is called cross relaxation. If one of the ions are at higher excited state than either of them were before, this is energy transfer up-conversion. In this work, ETU is a desired process and cross relaxation is considered a loss process [2]. Generally, losses caused by energy transfer, whose rate constants are dependent on the concentration of the dopant, are called concentration quenching. This phenomenon is a result of ions becoming so close together that

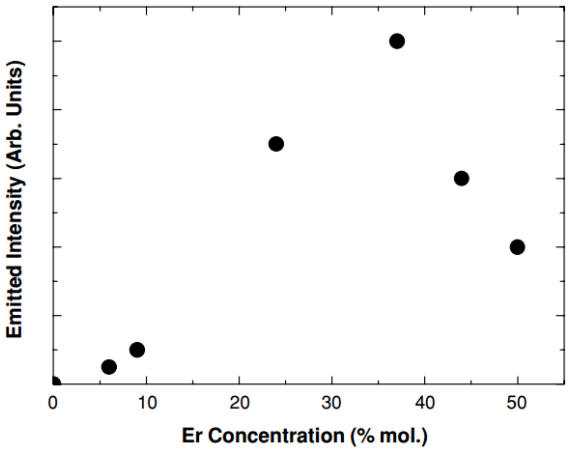

Fig 2.5: The integrated emission intensity of Er^{3+} ions, from 1.5-1.6μm excitation, as a function of Er^{3+} concentration [2].

they start to prefer cross relaxation over ETU, or even ESA. Figure 2.5 illustrates a concentration dependence plot of an erbium doped phosphor with 37.5% concentration as its peak.

2.5.1 Er^{3+} - Er^{3+} Separation Distance

As the number of luminescent centers that are doped into the host crystal increase, the closer the centers become. Therefore, if the crystal structure and doping concentration is known, then the average distance between doped ions can be determined. So, if R_{Er} is defined to be the average radial distance between erbium ions, then:

$$R_{Er} \cong 2\left(\frac{3V}{4\pi C_{Er} N}\right)^{\frac{1}{3}}, \tag{2.11}$$

Where V is the volume of the unit cell in the host crystal, C_{Er} is the doping concentration in decimal form, and N is the number of sites that an erbium ion can occupy per unit cell [6].

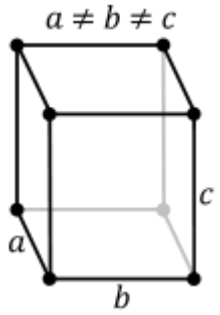

$$V = abc \tag{2.12}$$
$$a = \ 7.67\text{Å}^{[7]}$$
$$b = 11.41\text{Å}^{[7]}$$
$$c = 21.44\text{Å}^{[7]}$$
$$V = (7.67\text{Å}) * (11.41\text{Å}) * (21.44\text{Å}) = 1876.315\text{Å}^3$$

Gadolinium tungstate has an orthorhombic crystal structure, meaning that each dimension of its unit cell is a different length. The volume of this cell is the product of the length of each dimension (Eq 2.12). Above, the volume of the unit cell of $Gd_2(WO_4)_3$ is determined, and N is determined to be 2.

$$R_{Er} \cong 2\left(\frac{3(1876.315\text{Å}^3)}{4\pi(0.1)(2)}\right)^{\frac{1}{3}} = \ 26.1673\text{Å}, \text{ distance for 10\% } Er^{3+} \text{ concentration.} \tag{2.13}$$

Concentration (%)	Distance (Å)	Concentration (%)	Distance (Å)
15	22.8592	35	17.2347
20	20.7690	40	16.4844
25	19.2802	45	15.8497
30	18.1434	50	15.3027

2.8 Phonon Energy

As mentioned throughout Chapter 1, the phonon energies of a host lattice can seriously affect the luminescence process. This is because if the lattice has a very high phonon energy then it is more probable for the excited ion to emit a phonon rather a photon. The vibration of a crystal lattice is spoken in terms of phonons: a quanta of vibrational energy. For example, if a doped crystal with a phonon energy of 500 cm^{-1} is excited by radiation with 1000 cm^{-1}, then 2 phonons will be released instead of radiation, this is known as multi-phonon relaxation. As the phonon energy decreases, however, it becomes less likely that the excited state will emit phonons.

The $^4I_{13/2} \rightarrow {}^4I_{15/2}$ transition in erbium is a 6500 cm^{-1} change in energy, it is 10215 cm^{-1} for the $^4I_{11/2} \rightarrow {}^4I_{15/2}$ transition. The highest phonon energy for $Gd_2(WO_4)_3$ was found to be 1901 cm^{-1} [9]. This means that the GSA 1500 nm transition is 3.4 times the phonon energy and the GSA 980 nm transition is 5.4 times the energy. These values indicate that gadolinium tungstate has a low enough probability for multi-phonon relaxation to efficiently up-convert near infrared light.

References

[1] Auzel, F. “Materials and Devices Using Double-Pumped-Phosphors with Energy Transfer.” *Proceedings of the IEEE Proc. IEEE* 61.6 (1973): 758-86. Print.

[2] Suijver, J. Freek. “Upconversion Phosphors.” *Luminescence: From Theory to Applications.* Weinheim: Wiley-VCH, 2008. 133-177. Print.

[3] Strümpel, Claudia. “Application of Erbium-Doped Up-Converters to Silicon Based Solar Cells.” Diss. Konstanz, Univ., 2007. Print.

[4] Solé, J. García, L. E. Bausá, and D. Jaque. *An Introduction to the Optical Spectroscopy of Inorganic Solids.* Hoboken, NJ: John Wiley and Sons, Ltd, 2005. Print.

[5] Digonnet, M. “Rare-Earth-Doped Fiber Lasers and Amplifiers.” New York, Marcel Dekker Inc., 2001. Print.

[6] Cao, Chunyan, Hyun Kyoung Yang, Jong Won Chung, Byung Kee Moon, Byung Chun Choi, Jung Hyun Jeong, and kwang Ho Kim. “Hydrothermal Synthesis and Enhanced Photoluminescence of Tb3+ in Ce3+/Tb3+ doped KGdF4 Nanocrystals.” *Journal of Materials Chemistry* 21.28 (2011) 10342. Web.

[7] Madelung, Otfied, and Herbert Dittrich. “Gd2(WO4)3 Crystal Structure, Physical Properties.” *Ternary Compounds, Organic Semiconductors.* Berlin: Springer, 2000. Web.

[8] Lui, Zhixin, Qingyu Meng, Hongliang Liu. Chengbao Yao, Qinguo Meng, Wei Lie, and Weibo Wang. “Energy Tranfer and Electron-Phonon Coupling Properties in Gd2(WO4)3:Eu Phosphor.” *Optical Materials* 36.2 (2013: 384-89. Web.

CHAPTER 3

SYNTHESIS

3.1 Chemical Composition

Erbium doped gadolinium tungstate was prepared via co-precipitation method using 99.99% pure reagents; $Gd(NO_3)_3{\cdot}6H_2O$, $Er(NO_3)_3{\cdot}5H_2O$, and $Na_2WO_4{\cdot}2H_2O$. The chemical reaction equation is given below:

$$2Gd(NO_3)_3 + 3Na_2WO_4 \rightarrow Gd_2(WO_4)_3 + 6NaNO_3 \quad (3.1)$$

Where a percentage of the gadolinium is replaced with erbium. From the equation, it can be seen that the synthesis relies on a 2:3 molar ratio, so that if one requires a certain amount of gadolinium tungstate they would need to mix twice (2) that molar amount of gadolinium nitrate with three (3) times the molar amount of sodium tungstate.

Approximately 2 grams of gadolinium tungstate is needed. Two grams were by the formula weight (FW) of gadolinium tungstate, 1058.013 g/mol, (Eq 3.2).

$$\frac{2\text{g}}{1058.013\text{g/mol}} = 0.00189\text{mol} \approx 0.002\text{mol}. \quad (3.2)$$

Therefore, 0.004 mol of a gadolinium and erbium nitrate mixture needs to be mixed with 0.006 mol of sodium tungstate.

$$0.006\text{mol} \cdot 329.85\text{g/mol of } NaWO_4, = 1.9791\text{g} \quad (3.3)$$

The sodium tungstate was dissolved into 30 mL of deionized water, and was titrated into a 10 mL mixture of erbium and gadolinium tungstate in deionized water. The erbium and gadolinium compounds can be more precisely mixed if they are already in an aqueous solution.

$$\#\text{mol of Gd} + \#\text{mol of Er} = 0.004\text{mol per } 10\text{mL}, \quad (3.4)$$

so they can be made into a solution with a concentration of 0.0004 mol/mL.

Table 3.1

% Er	mL Gd	mL Er	Total mL	mol Gd	mol Er	Total mol	mL WO_4
0	10	0	10	0.004	0	0.004	30
10	9	1	10	0.0036	0.0004	0.004	30
15	8.5	1.5	10	0.0034	0.0006	0.004	30
20	8	2	10	0.0032	0.0008	0.004	30
25	7.5	2.5	10	0.003	0.001	0.004	30
30	7	3	10	0.0028	0.0012	0.004	30

Table 3.1 presents a total amount of milliliters needed, but 50mL of aqueous $Gd(NO_3)_3$ and 15mL of aqueous $Er(NO_3)_3$ were made, along with the 180mL of aqueous Na_2WO_4.

50mL · 0.0004mol/mL = 0.02mol, 0.02mol · 451.36g/mol = 9.0272g to 50mL gadolinium nitrate.

15mL · 0.0004mol/mL = 0.006mol, 0.006mol · 443.35g/mol = 2.6601g to 15mL erbium nitrate.

6samples · 1.9791g per sample = 11.8746g for 180mL sodium tungstate.

Then, due to insufficient concentration quenching of our samples, 35%, 40%, 45%, & 50% samples were prepared.

25mL · 0.0004mol/mL = 0.01mol, 0.01mol · 451.36g/mol = 4.5136g to 25mL gadolinium nitrate.

20mL · 0.0004mol/mL = 0.008mol, 0.008mol · 443.35g/mol = 3.5468g for 20mL erbium nitrate.

4samples · 1.9791g per sample = 7.9164g for 120mL sodium tungstate.

Table 3.2

Batch 1			
Chemical	mL H_2O	Theoretical (g)	Actual (g)
$Gd(NO_3)_3{\cdot}6H_2O$	50	9.0272	9.027
$Er(NO_3)_3{\cdot}5H_2O$	15	2.6601	2.663
$Na_2WO_4{\cdot}2H_2O$	180	11.874	11.876
Batch 2			
$Gd(NO_3)_3{\cdot}6H_2O$	25	4.5136	4.515
$Er(NO_3)_3{\cdot}5H_2O$	20	3.568	3.548
$Na_2WO_4{\cdot}2H_2O$	120	7.9164	7.925

3.2 Synthesizing $Gd_2(WO_4)_3:Er^{3+}$ via Co-Precipitation Method

Traditionally, tungstates are synthesized by the solid-state reaction method, but this process has a few disadvantages. The solid-state method needs high calcination temperatures (1100-1200°C), and it produces crystals with a large particle size and irregular morphologies. Hydrothermal and Penchini methods also have drawbacks, such as complicated procedure and long preparation period. Therefore, the samples were prepared using the co-precipitation method due to the ease of synthesis, low annealing temperatures, and consistent crystal morphology.

In this procedure, Solution A refers to the aqueous mixture of $Gd(NO_3)_3$ and $Er(NO_3)_3$ in the appropriate amounts pertaining to the specified doping concentration. Each step is the same for every sample regardless of the percentage of erbium, except for the making of Solution A. Solution B, by contrast, is the aqueous solution of Na_2WO_4, which is identical for all samples.

1. Solution B is added drip-wise at a rate of 1mL/min (where Solution B is 30mL) into Solution A under constant stirring. When Solution B contacts Solution A, it immediately forms a precipitate, $Gd_2(WO_4)_3$, and an aqueous byproduct, $NaNO_3$, nitratine. The mixture AB is kept under stirring for another 30min to ensure that all the chemicals have reacted with each other.
2. The AB mixture is centrifuged at 1000rpms for 20mins to concentrate the solid, insoluble gadolinium/erbium tungstate, but keep it loose enough to wash out the nitratine that is trapped in the solid. The mixture is centrifuged and washed three (3) times, then centrifuged a final time at 4000rpm for 20mins.
3. The precipitate, which should be all that is left, is dried in an oven at 90°C for 3hrs. Afterward, the dried precipitate is ground down into a find powder in order to mix the erbium tungstate dominate areas with the gadolinium tungstate dominate areas.
4. The powder is placed into a crucible and annealed for 5hrs at 900°C. The annealing process energizes the gadolinium tungstate molecules and the erbium tungstate molecules and then allows them to cool slowly and the erbium to settle into the optical centers surrounded by the gadolinium. After

annealing the precipitate is ground again to ensure a homogenous distribution.

5. The annealed erbium doped gadolinium tungstate powder is pushed, as opposed to pressed, through a disc pill dye to create a flat disc that can be securely placed on optical mounts. If the powder is pressed with any substantial pressure, the pill press will leave the disc with an inhomogeneous surface; some areas are nice and matte and some have a metallic shiny surface, which can throw off optical experiments. Therefore the powder in the dye is pushed through to form a disc. After the disc is carefully pushed through, in hopes that it doesn't break, it is annealed again to harden the disc form.

Even though the same weight of powder is pushed through the pill press, the resulting disc might be of varying thickness, due to the difference in densities between different concentrations of erbium. However, the thickness doesn't matter depending to the type of optical mount in use. What matters is that the surface be uniformly matte, which it should be as long as the metal pill dyes don't apply too much pressure or torque to the powder.

CHAPTER 4

EXPERIMENTAL METHODS

4.1 Equipment

During synthesis, ACROS Organics Sodium tungstate dehydrate, ACROS Organics Erbium(III) nitrate pentahydrate, and Alfa Aesar Gadolinium(III) nitrate hydrate, with a purity of 99.9% each, were mixed in the processes described in Chapter 3. The aqueous sodium tungstate solution was titrated using a Harvard apparatus 11 Plus Syringe Pump. The precipitate was centrifuged using a Sorvall Legend XTR Centrifuge. The annealing process was carried out in a Zircar Hot Spot 110 Furnace and the discs were formed using a MTI Desk-Top Powder Presser. X-ray diffraction studies were performed on a PANalytical X'Pert Pro powder X-ray diffractometer with Cu $K\alpha_1$ radiation (λ = 1.5406Å) at the University of Georgia with the help of Dr. Feng Liu.

During experimentation, an Opto Engine LLC 1470 nm 800 mW scientific laser with PSU-H-LED power supply was used as the external 1500 nm excitation source. The 980 nm source was a ThorLabs L975P1WJ Laser Diode mounted onto the ThorLabs LDTCLDM9 Temperature Controlled laser diode mount, which was controlled using the ThorLabs Thermoelectric Temperature Controller (TED200C) and Laser Diode Controller (LDC200C). These two sources were used in conjunction with a Jobin Yvon FluorMax-3 Spectrometer, in order to conduct visible spectroscopy. A Horiba Jobin Yvon Fuorlog iHR320 Spectrometer was used to carry out IR spectroscopy. All spectroscopic data were collected and analyzed using Horiba's FluorEssence 3.5 software.

4.2 Set-up

Up-conversion spectra were gathered by running spectroscopic tests on differently doped samples using external laser sources. The samples were swiveled on a mount to find the angle that had the most intense emissions. While at this angle, tests were run with various current strengths flowing through the sources. This varies the power coming out of the sources. When sources or samples are changed, the new, most intense angle had to be found again to ensure that

only the most intense light was being studied. Down-conversion and IR spectra were obtained in the Fluorolog iHR320 spectrometer using internal sources and sensors. Figure 4.1 illustrates the basic setup for conducting spectroscopic studies. The samples are placed at a certain angle to the excitation beam so that the most intense light can fall onto the rotating grating. The grating then rotates so that the CCD can detect the amount of light per unit of wavelength. The light must pass through an optical filter in order to keep from saturating the detector with excitation light.

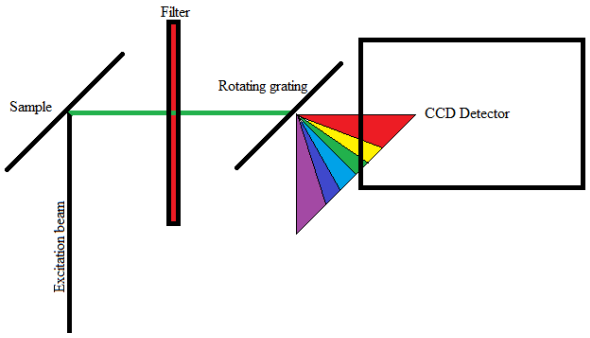

Fig 4.1: Basic schematic of spectroscopic setup.

4.3 Analytical Methods

After acquiring data, certain transforms were applied to it in order to discuss the results in more physical terms. Firstly, except for the power dependent studies, the percent concentration was transformed into distance per erbium ion. The power dependent studies aren't dependent on concentration so it doesn't matter if we label them using percentages. As described before, the erbium concentration is directly proportional to the average distance between erbium ions, i.e. the higher the concentration, the closer the erbium ions. Figure 4.2 depicts how erbium separation varies with concentration. This transform is used to make the finding easier to conceptualize, but graphs in terms of concentration are also provided.

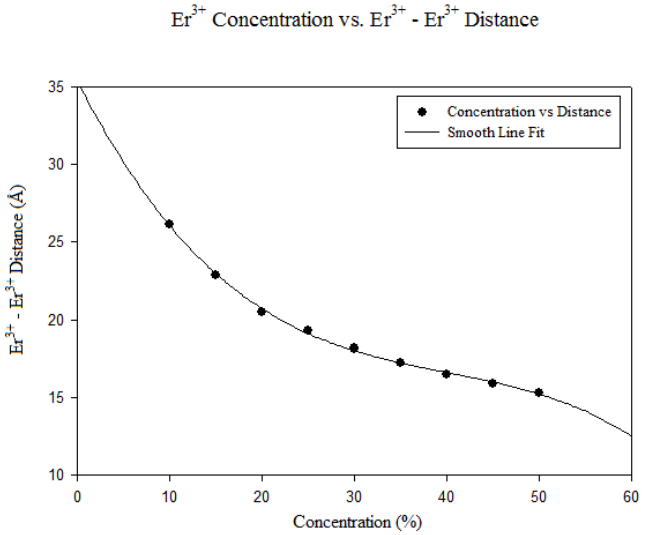

Fig 4.2: Graph depicting how the Er^{3+} separation distance changes with increasing concentration, according to Eq 2.11.

Another transform that was performed on the double log graphs. Instead of them being dependent on the log of the power, they are dependent on the log of the current passing through

the excitation source. This was done because the power was unknown but is proportional to the applied current:

$$I \propto P^n, I \propto C^n, \text{ where } C \text{ is the current} \tag{4.1}$$

$$C \propto P, \tag{4.2}$$

It is noted that this might be a source of error, especially concerning the photon count of the red emissions from 980 nm excitation (Fig 5.9(d)).

CHAPTER 5

RESULTS

5.1 Structural Characterization

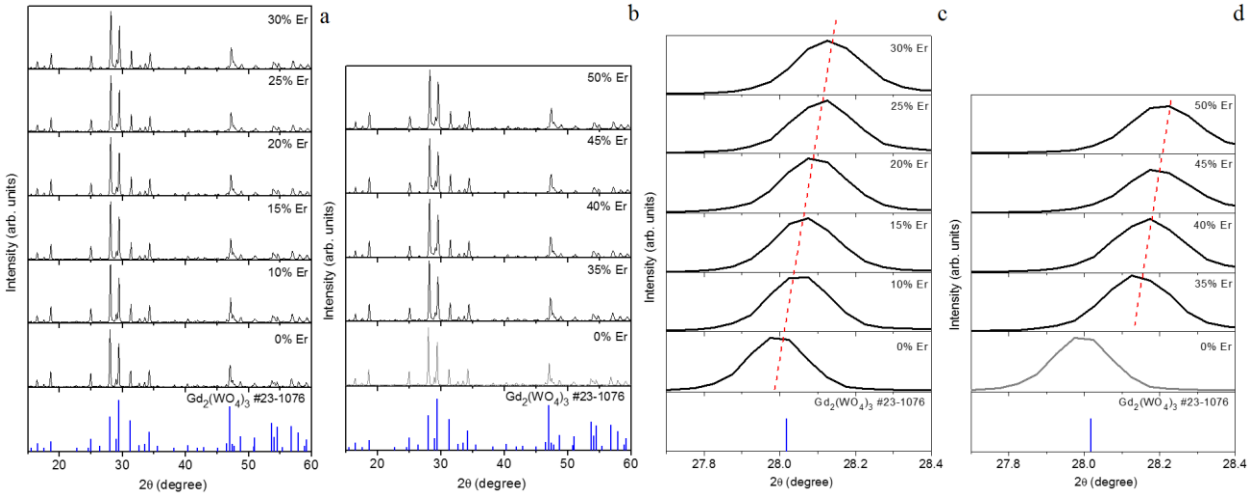

Fig 5.1(a,b): X-ray diffraction studies of samples of $Gd_2(WO_4)_3$: Er^{3+}. Fig 5.1(c, d): The peak located just over 28 degrees shifts as the erbium concentration increase.

Figures 5.1(a & b) show x-ray diffractograms from the Er^{3+} doped $Gd_2(WO_4)_3$ samples that were used in this thesis. All of the graphs illustrate that the samples are a match to the XRD standard, meaning the crystal structure of our samples are the same as the structure of $Gd_2(WO_4)_3$. Figures 5.1(c & d) focus on the peak located just over 28.0 degrees. These figures track the shift the peak goes through as the concentration of erbium was increased. The consistent linear shift says that neither the doping nor the labels are incorrect. The peak moved to the right due to how much smaller erbium is to gadolinium. Since erbium replaced more and more gadolinium as concentration increased, the lattice constants got smaller, causing a shift in the graphs. The samples in this thesis are proven to be consistently doped $Gd_2(WO_4)_3$:Er^{3+}.

5.2 Concentration Effects

The figures below are drawn to showcase how certain atomic transitions changed in intensity when the distance between the luminescence centers were changed. When concentration of the luminescent ions are increased, the distance between the ions are decreased, when this happens certain transitions occur more often and others less often. Testing for concentration dependence can reveal which type of UC processes are taking place. Graphs were made in terms of both distance in angstroms and percent erbium concentration.

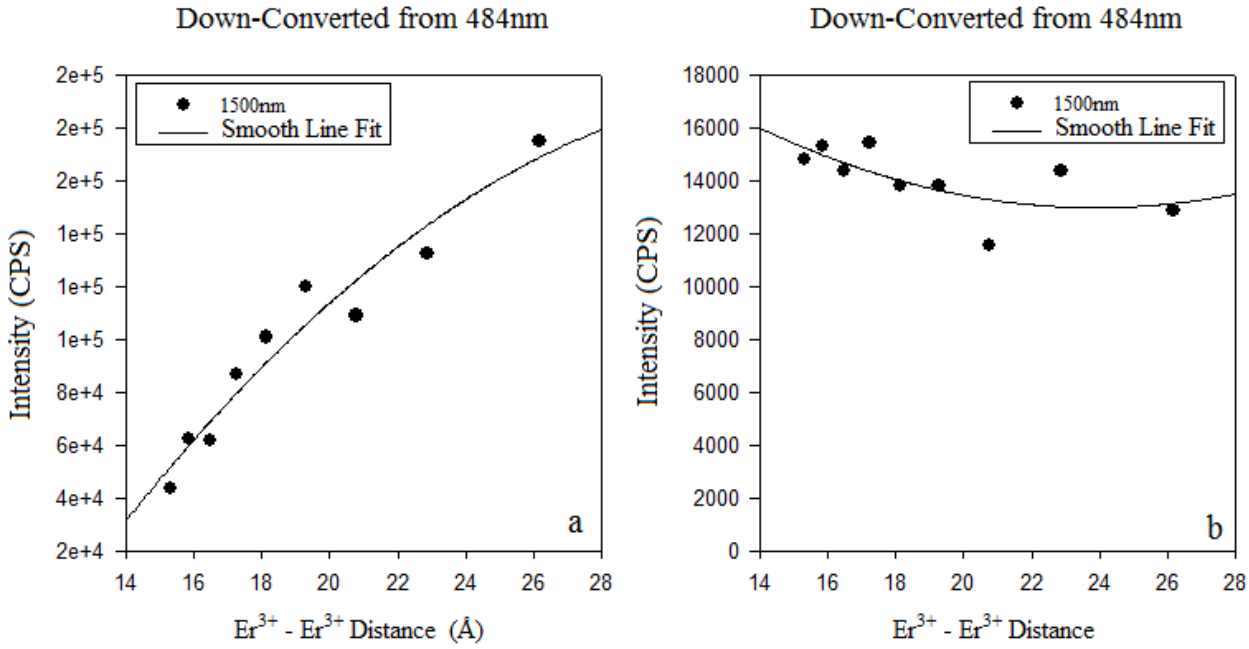

Fig 5.2(a, b): Depicts the dependence of erbium ion distances on the 980 nm and 1500 nm emissions. (a) shows strong dependence on how close the Er^{3+} ions are to each other, while (b) shows very little change in average intensity.

When an erbium ion absorbs a photon with a wavelength of 484 nm, one of its ground state electrons is excited to the $^4F_{7/2}$ energy level and from there can emit at most three (3) 1500 nm photons or two (2) 980 nm photons. It can be seen from Figure 5.2(a) that less and less 1500 nm photons are emitted when erbium ions get closer. The down-conversion process quenches very rapidly as concentration increases. However, the 980 nm emissions undergo very little change, but this is most likely due to the fact that only two photons have to be successfully emitted instead of three.

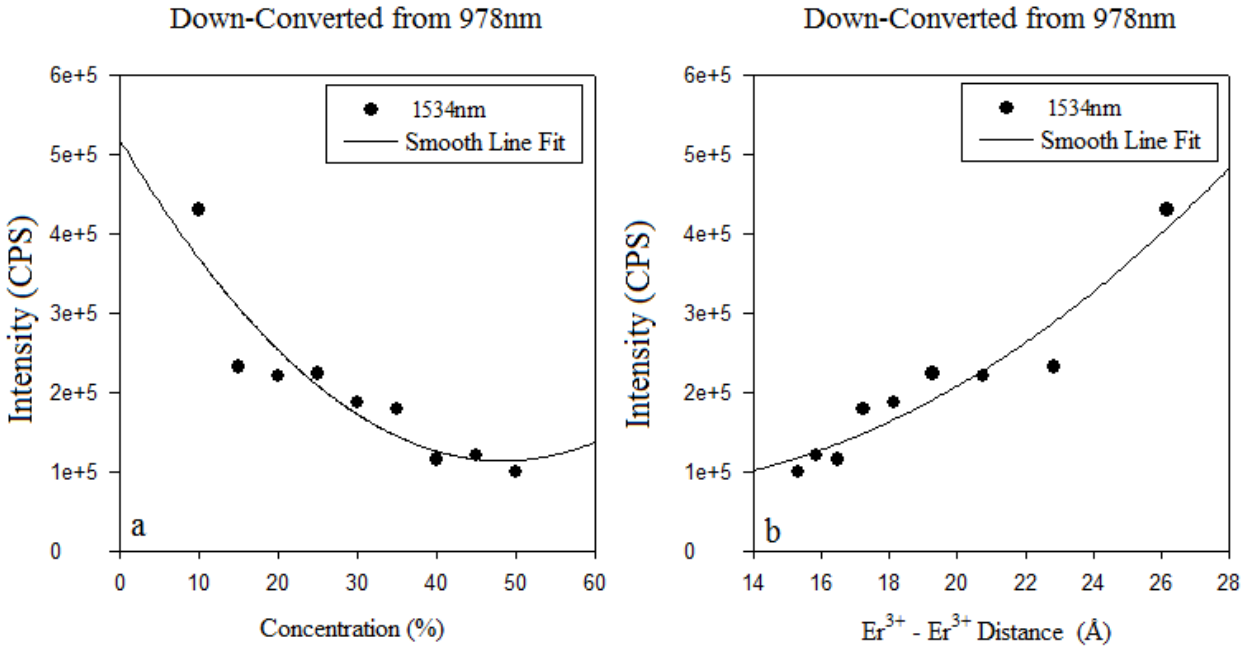

Fig 5.3(a, b): Concentration and distance dependent plots of intensity of the $^4I_{13/2} \rightarrow {}^4I_{15/2}$ transition when excited with 980 nm photons.

There is a strong concentration quenching apparent in Figures 5.3(a & b). When they are highly concentrated and close to each other, the ions are more likely to CR the energy without emitting radiation. Both down-conversion results point towards strong concentration quenching connected with 980 nm producing the $^4I_{13/2} \rightarrow {}^4I_{15/2}$ transition.

Figures 5.4(a & b) and 5.5(a & b) depict UC dependence on erbium ion separation, and they look nothing like the four previous graphs. Fig 5.4(a & b) show peaks in their dependence curves. These peaks indicate a sweet-spot where the erbium ions are close enough to talk but not close enough to cross relax. Fig 5.5(a) shows a peak while Fig 5.5(b) shows a near linear inverse relationship. The reason for the stark difference could be due to the power of the polynomial describing the line of best fit. The line in Fig 5.5(b) is described with 2nd power polynomial, then it might require a 4th power polynomial to accurately describe the best line of fit.

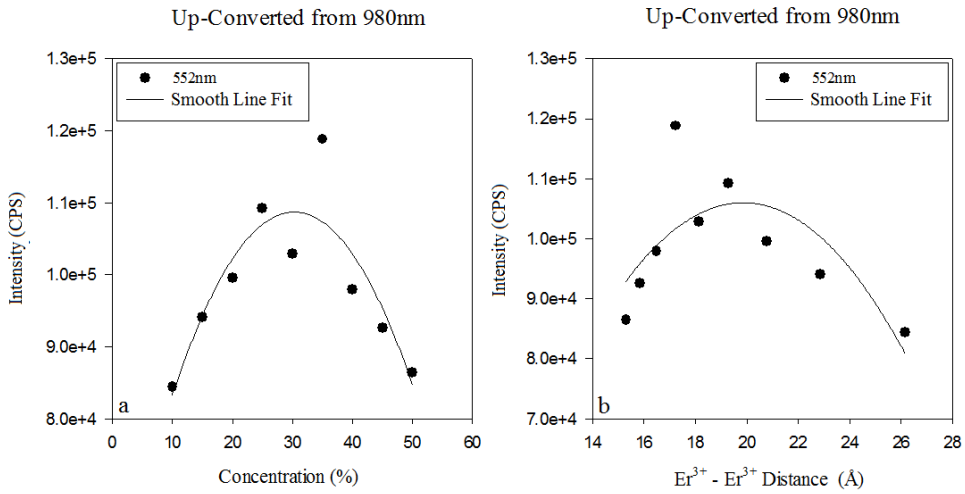

Fig 5.4(a, b): Depicts how the intensity of the $^4S_{3/2} \rightarrow {}^4I_{15/2}$ transitions under 980nm excitation changes as concentration and erbium ion separation are changed. The peak in the graphs indicate the presence of a concentration that spaces the erbium ions just far enough away to most efficiently convert 980 nm NIR light into 552 nm green light.

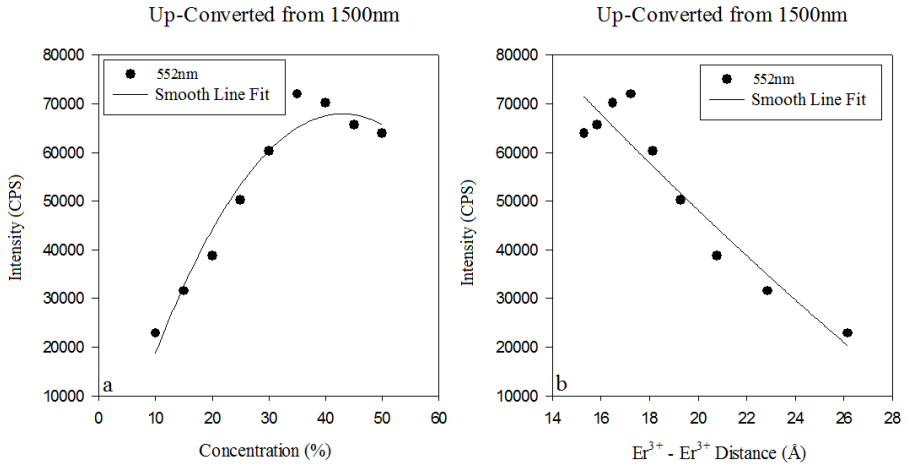

Fig 5.5(a, b): The intensity of the $^4S_{3/2} \rightarrow {}^4I_{15/2}$ transitions under 1500 nm excitation changes as concentration and erbium ion separation are changed. The peak in (a) indicate the presence of a concentration that spaces the erbium ions just far enough away to most efficiently convert 1500 nm IR light into 552 nm green light. Fig (b) shows either a negative linear relationship or a very narrow peak with a very precise concentration.

5.2.1 Spectrographs

Below, figures 5.6 and 5.7, examples of the emissions spectra used to characterize the concentration dependence. On the next page there are spectrographs comparing the different up- and down-conversions under investigation. Figure 5.8 depicts the 900-1700 nm emission spectrum of 484 nm DC. The black line shows the full 900-1700 nm spectrum with the entrance and exits slits on the spectrometer partially opened. The red line shows the 940-1050 nm range of the spectrum with entrance and exit slits all the way open, this magnifies the signal. It can be seen that the 1500 nm signal is a lot more intense that the 980 nm signal, even when it is magnified the 980 nm signal still pales in comparison.

Figure 5.9 compares the 1400-1700 nm range of the emission spectrum of 484 nm and 978 nm down-conversion. The 978 nm (black) DC produces a more intense 1500 nm emission than 484 nm (blue) DC. This is due to 484 nm DC having many different avenues to emit lower energy photons, while 978 nm can only DC to 1500 nm. Figure 5.10 compares the 500-800 nm range of the emission spectrum of 980 nm and 1500 nm up-conversion. The 980 nm (black) UC emission shows a brighter green emission compared to 1500 nm UC, but a dimmer red emission. The 1500 nm UC has a more intense red emission due to the $^4F_{9/2}$ state needing closer to an integer number of photons to populate, making it a more probable transition.

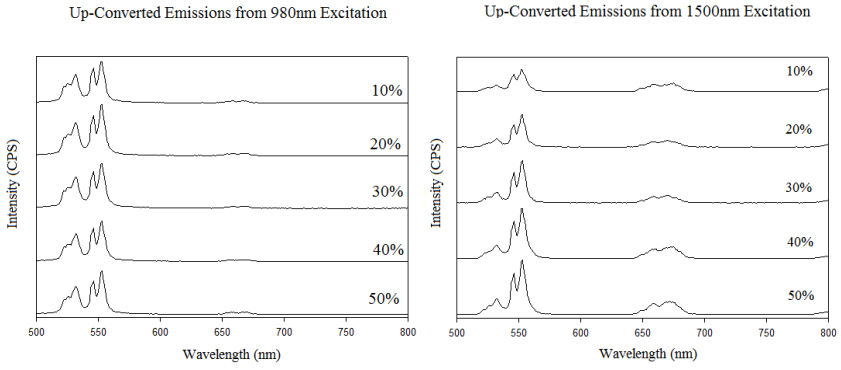

Fig 5.6: 500-800 nm emissions spectra when the samples were excited by 980 nm and 1500 nm.

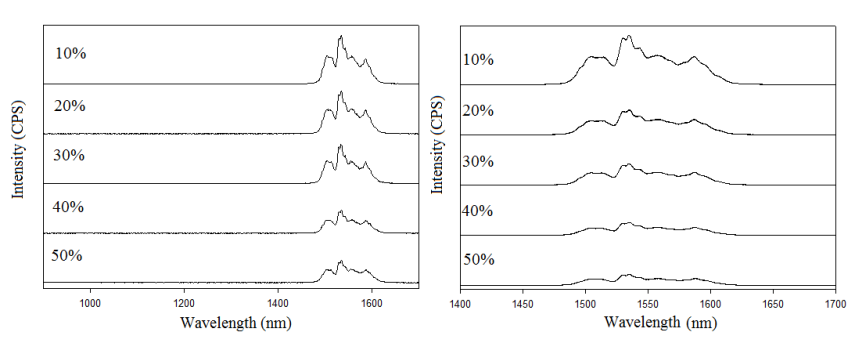

Fig 5.7: First, 900-1700 nm emissions spectra when DC 484 nm photons. Second, 1400-1700 nm emissions when DC 978 nm photons.

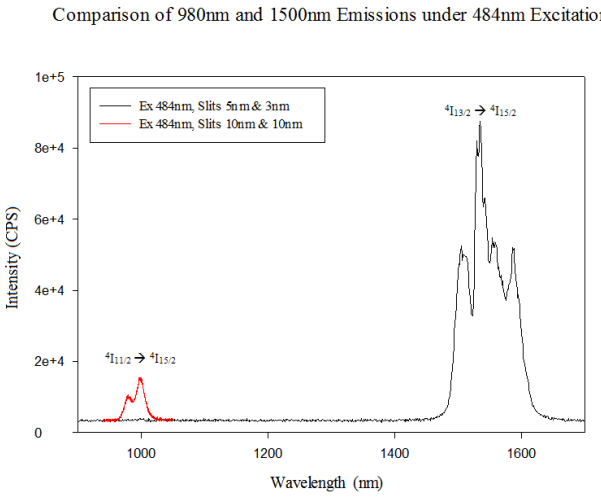

Fig 5.8: Compares the intensity of the 980 nm and 1500 nm transitions when down-converted from 484 nm. Red line indicates the 980 nm peak when the spectrometer has its entrance and exit slits wide open, magnifying the peak.

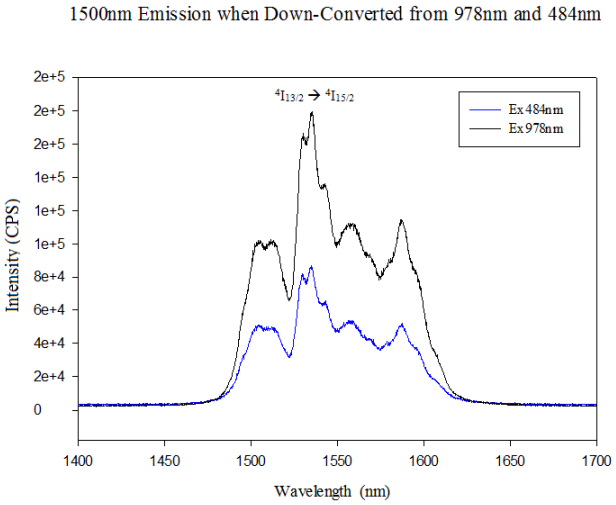

Fig 5.9: Compares the 1500 nm emissions of down-converted 484 nm and 980 nm. It shows that 980 nm produces the most intense emission of 1500 nm light.

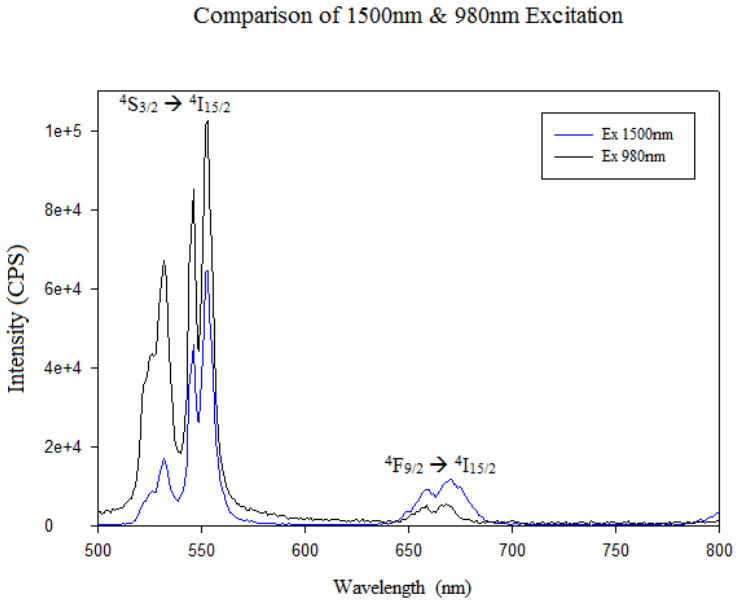

Fig 5.10: Compares the intensity of the range of emitted light (500 nm – 800 nm) when up converted by 980 nm (black line) or 1500 nm (blue line) light. It shows that although 980 nm excitation produces a more intense green emission, the red emission is less efficient.

5.3 Power Dependence

Figure 5.11 demonstrates how the intensity of the emission spectra is proportional to incident power. As described in Section 2.4, the slopes in figures 5.13(a, b, c, & d) represent the number of photons used in order to emit a photon from the transition being tested. Data point for these graphs were compiled from spectra like the ones in figure 5.11. Figure 5.12 shows a sample of the graphs shown on the next page. The samples illustrates that three 1500 nm photons are used to produce a 552 nm photons. The $^4S_{3/2} \rightarrow {}^4I_{15/2}$ (552 nm) and the $^4F_{9/2} \rightarrow {}^4I_{15/2}$ (670 nm) transitions are of importance in Fig 5.13. As concentration increases, the number of photons used by the erbium ion to excite a particular state will change depending on what processes are used to UC. The number of photons used for the multi-photon excitation are graphed in the next section to shed light on any possible patterns.

It needs to be noted, though, that Fig 5.13(d) depict results that do not make physical sense. The slopes of these graphs fall below 2, saying one low energy can be up-converted to one high energy photon, which is impossible. Therefore these results are discussed no further, except to point out that the power to current transform might be the cause of the error.

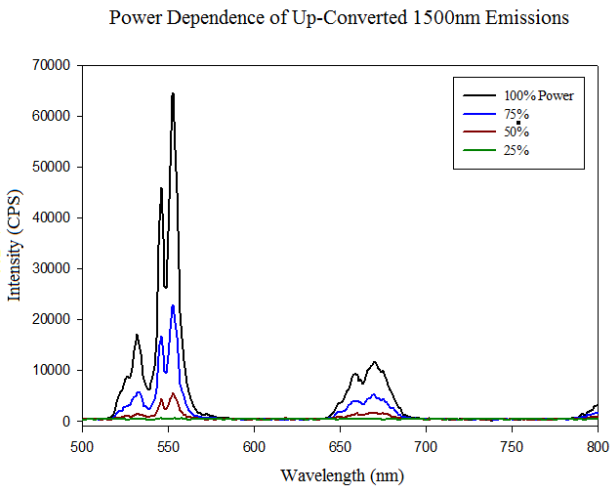

Fig 5.11: Over-layed spectra showing how emission intensity decreases with a decrease in power.

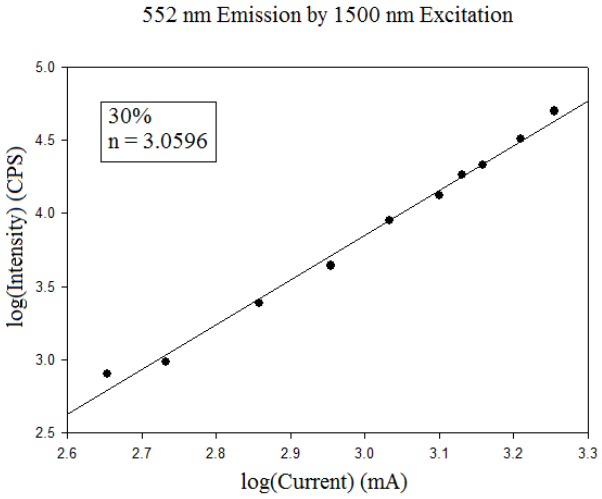

Fig 5.12: A sample double logarithmic graph of current versus intensity. Here it is found, the 30% erbium concentration sample uses three 1500 nm photons to produce a 552 nm photon.

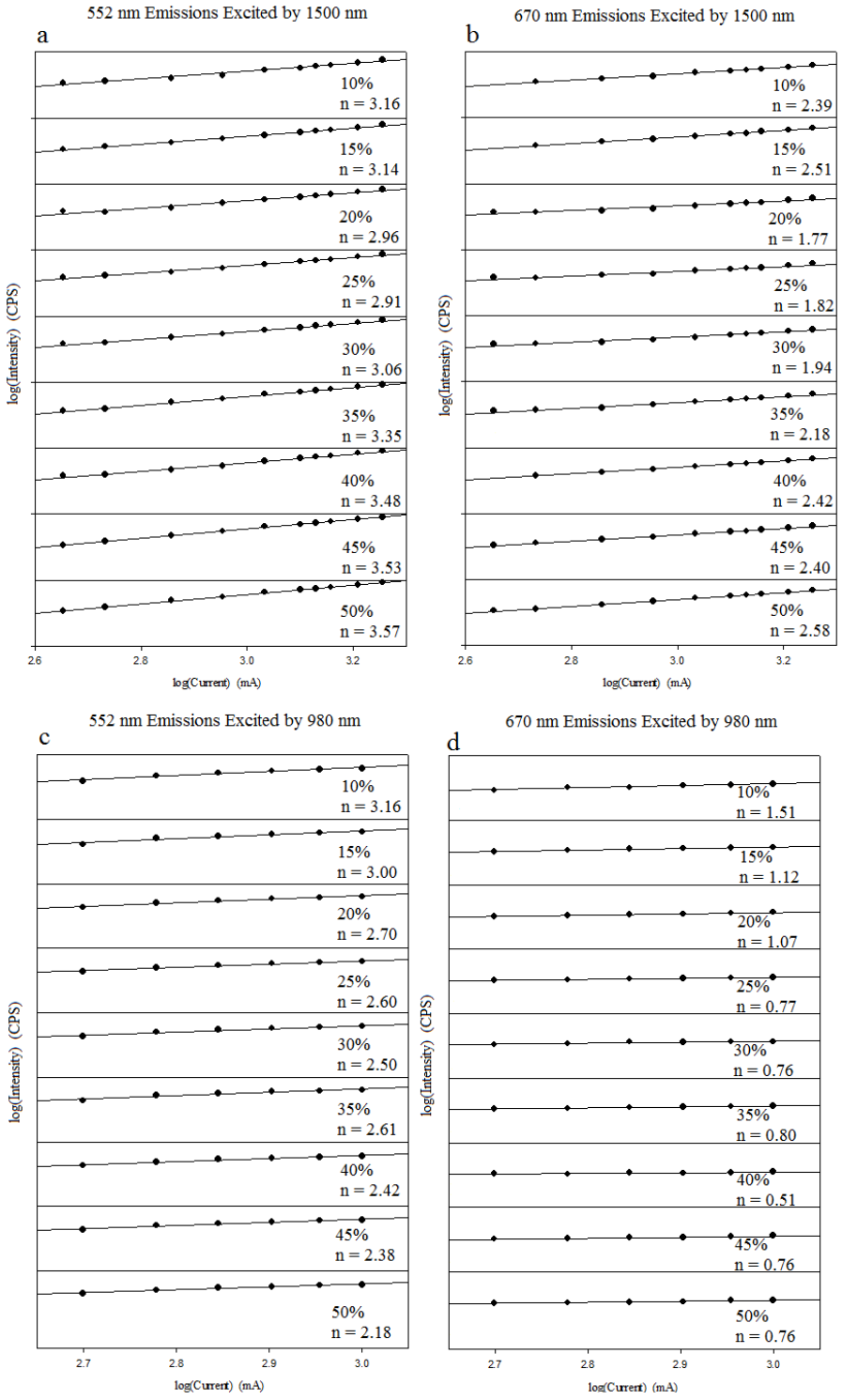

Fig 5.13: Double log current versus intensity graphs depicting how the intensity of red or green emission, under either 1500 nm or 980 nm excitation, changes with the current applied to the excitation source. The results show a linear relationship, and the slope of the line is the number of photons used in the process. Although the results from (b) agree that it take two 1500 nm photons to make a red photon, (d) is nonsensical, implying that 1 low energy photon can create 1 high energy photon.

5.4 Multi-photon Excitation

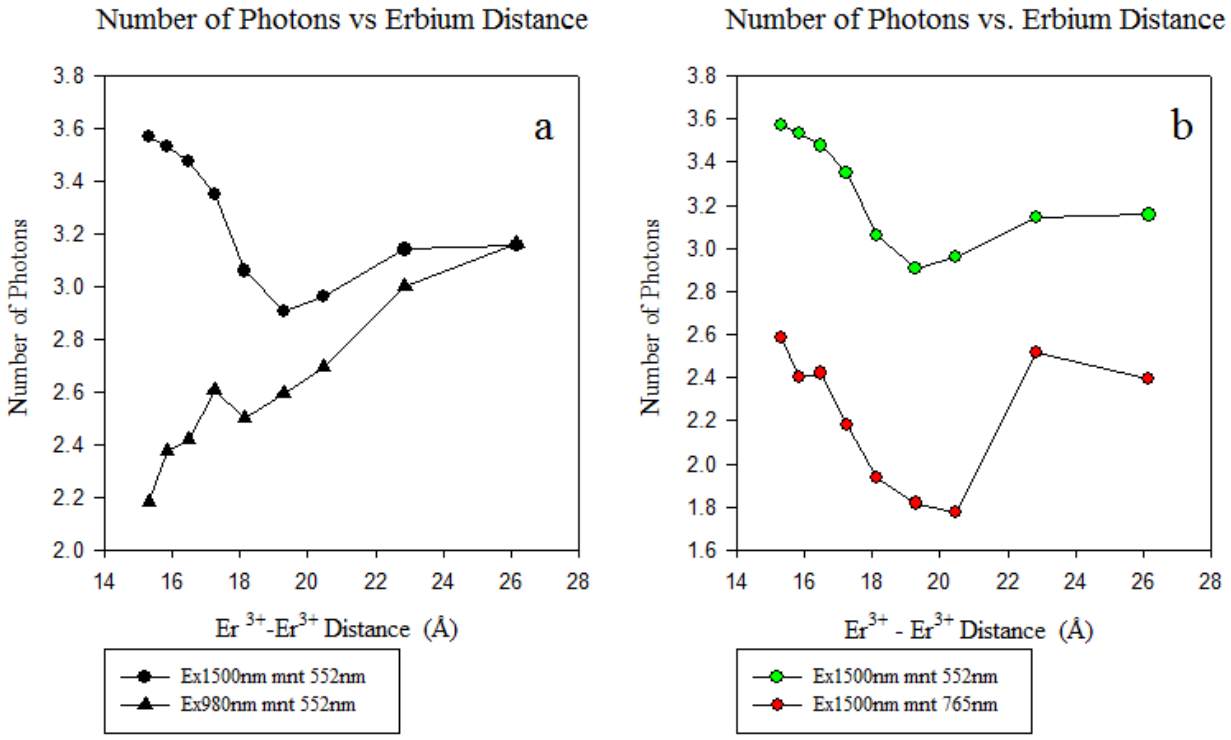

Fig 5.14: Photon number versus separation distance. Instead of speaking in terms of slopes per concentration, they are transformed into number of photons per distance between erbium ions for simplicity. It can be seen that 1500 nm excitation has a minimum of photons for green transitions, where 980 nm excitation shows an almost linear increase in the number of photons as distance increases.

Above, Figure 5.14 compares the photon count of either (a) the same transition under different excitations, or (b) the same excitation monitoring different transitions. In Fig 5.14(a), the 1500 nm plot shows a minimum at 25% Er^{3+}, while the 980nm plot shows a near linear quenching as the ions get further away. Both 1500 nm plots in Fig 5.14(b) contain a minimum. When investigating 552 nm emission, the minimum is located at 25%, but when 765 nm is being investigated, the minimum is now at 20%. Also, the photon numbers agree with the photon count taken earlier in Section 2.5; 3 photons for 1500 nm to emit 552 nm, 2 photons for 1500 nm to emit 765 nm, and 2 photons for 980 nm to emit 552 nm. It can be seen in Fig 5.14(a) that, depending on the concentration, its take 980 nm either 2 or 3 photons to emit 552 nm, meaning that the processes becomes more inefficient as concentration decreases. 1500 nm ranges from 2 to 3 photons to UC to red, and 3 to 4 photons to up convert to green. Figure 5.16 illustrates where these extra photons may be located.

5.5 Mechanisms

Figure 5.16 is the overlaying of 5.4(a) and 5.5(a). Figures 5.16(e & f) showcase how the different up-conversion processes can change the number of used photons. Fig 5.16(e) shows that the $^4I_{9/2}$ state non-radiatively decays to the $^4I_{11/2}$ state where an extra photon is needed to excite to $^4F_{9/2}$. Another non-radiative decay re-populates the $^4I_{9/2}$ state and then another photon brings the electron up to the $^2H_{11/2}$ state which normally decay to the $^4S_{3/2}$ state to emit a 552 nm photon. Fig 5.16(e) also shows how the extra photon can cause the 765 nm emission to go from a 2 to a 3 photon process. It can be assumed from (e) that the $^4F_{9/2}$ energy level (654 nm emission) would always need 3 photons to be populated. Fig 5.16(f) depicts the 980 nm process using and extra photon unnecessarily between $^4I_{13/2}$ and $^4I_{9/2}$. The extra photon illustrates the inefficiency of using 3 photons to emit a 552 nm photon.

Comparing figures 5.14, 5.15 and 5.16, at low concentrations the erbium ions prefer to add an inefficient cycle of non-radiative decay, ESA, then non-radiative decay again to the starting energy level. These cycles are only interrupted as concentration increases. It can be seen that the UC of 980 nm photons to 552 nm photons uses the most (3) photons when concentration is low and Er^{3+} ions are separated. As Er^{3+} concentration increases, the number of 980 nm photons decreases linearly to 2 photons. This indicates that 980 nm UC depends on the ETU of other nearby ions. When considering figure 4, this means that the only reason the intensity decreases as concentration increases is due to concentration quenching.

1500 nm UC does not show the same trend as 980 nm UC, meaning that it is dependent on different mechanisms. The UC of 1500 nm photons starts to use less photons as concentration increases to 20-25%, meaning that ETU is the dominant process, then rapidly starts using more photon as concentration increases to 50%. This indicates that the ions are close enough to no longer prefer to ETU their energy, but rather cross relax it to a lower energy level of an excited neighbor, resulting in a loss of energy. Consulting figure 5.15, even though cross relaxation become the dominant process, the intensity of the 552 nm emission increases until 40% erbium concentration, meaning that the increase in number of photons used in UC also increases the number of photons emitted.

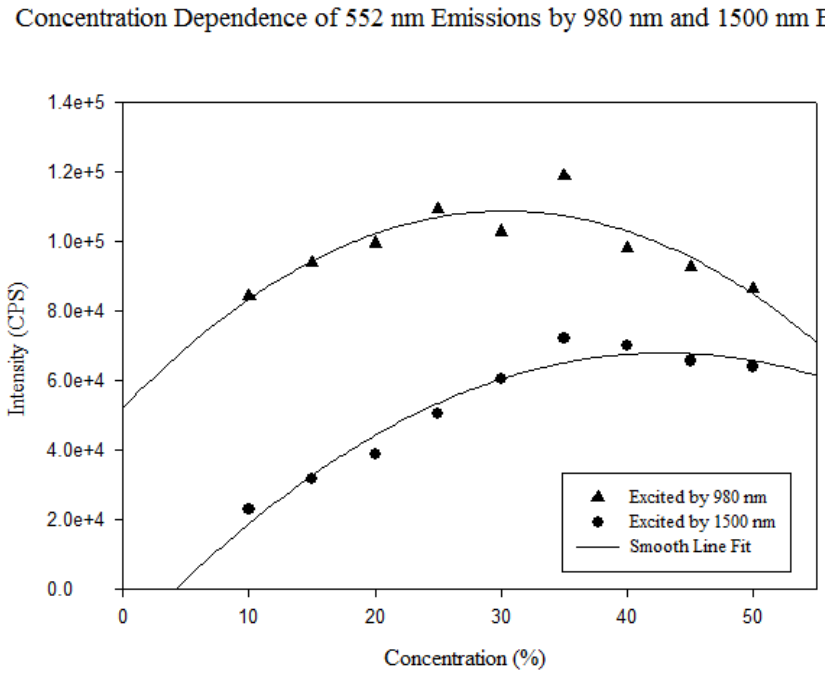

Fig 5.15: Overlay comparison of the concentration dependence on the 552 nm emissions when UC 980 nm (triangles) and 1500 nm (circles) photons.

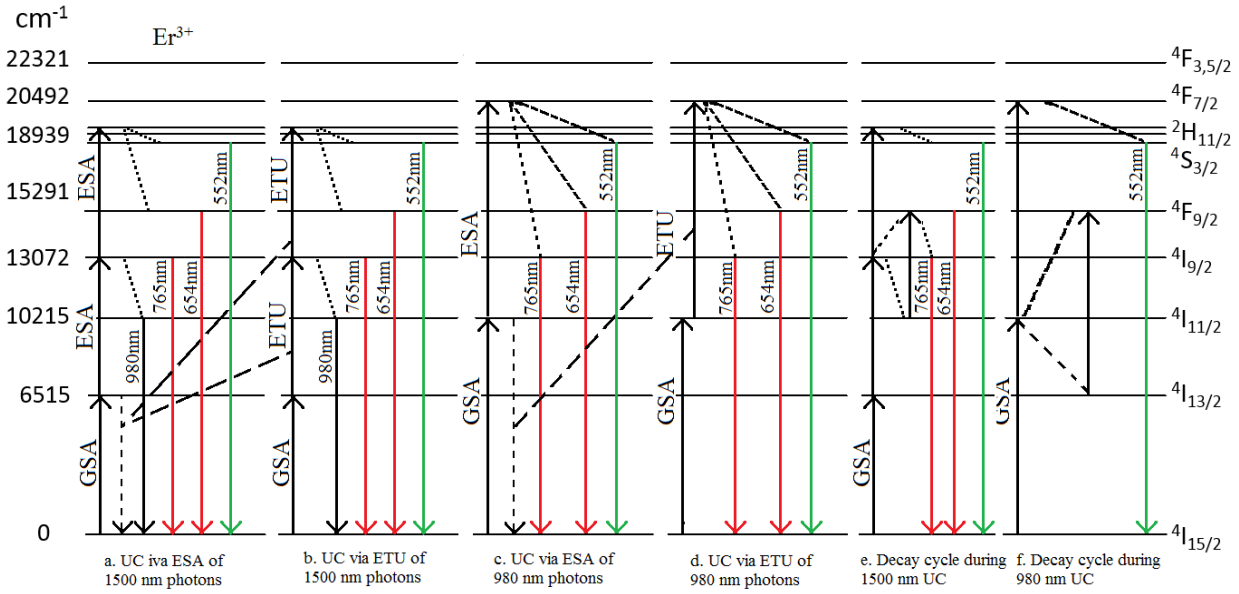

Fig 5.16(a-d): Illustrates the possible ways to UC 1500 nm and 980 nm radiation. Fig 5.16(e, f) shows two unnecessary non-radiative decays that cause the UC process to be less efficient. . Fig 5.16(e): Depicts how the $^4S_{3/2} \rightarrow {}^4I_{15/2}$ transition can change between a 3 and a 4 photon processes under 1500 nm excitation.
Fig 5.16(f): Depicts how the $^4S_{3/2} \rightarrow {}^4I_{15/2}$ transition can change between a 2 and a 3 photon processes under 980 nm excitation.

CHAPTER 6

CONCLUSIONS

In this thesis, samples of gadolinium tungstate doped with varying amounts of erbium ions were structurally and spectroscopically analyzed. The structural data from the XRD studies testify to the purity of the crystal structures of the sample due to no phase change being observed up to 50% erbium. Also, the shift in the XRD data corresponds to the consistent decrease in the lattice constants indicating that erbium is being consistently increased, since more, tinier erbium ions are replacing the larger gadolinium ions.

Though, some error may have been made during experimentation, or during calculations, the results are very revealing as to what mechanisms may be involved in the up-conversion processes. The efficiency alone quantifies erbium doped gadolinium tungstate as a strong contender for applications such as solar cell up-converters.

The up-conversion concentration in figures 5.4 & 5.5, showcase peaks that suggest a most efficient concentration for up-converting 1500 nm and 980 nm incoming radiation. From Fig. 5.4, the maximum of the curve fit hovers around 20% concentration for both (a) & (b). Fig 5.5(a) locate its curve maximum near 45%, however, (b) does not showcase any peaks or maxima. As stated before Fig 5.5(b) may need a higher power polynomial to adequately describe its line of best fit.

The power dependent graphs reveal the slopes of each concentration under different excitation, monitoring different emissions. The slopes are then plotted by erbium distance versus photon number. The $^{2}H_{11/2}$ energy level ranged from requiring 3 to 4 1500 nm photons or 2 to 3 980 nm photons. The $^{4}I_{9/2}$ energy level ranged from a 2 to 3 1500 nm photon processes. The possible up-conversion mechanisms are illustrated in figure 5.16, showing how the efficiency can be undermined if there is too much concentration. As concentration increases, erbium uses less 980 nm photons to produce 552 nm photons mainly via ETU, however after 30% concentration the 552 nm emission starts becoming quenched. Erbium ions use less 1500 nm photons to UC as concentration increases to 25% due to ETU, then dominant process becomes cross relaxation. Until 40% erbium concentration, the cross relaxation process still produces more 552 nm emissions, when the emissions die due to concentration quenching.

Future work could be done to calculate the lifetime of the excited states and the quantum efficiency of the processes. Also, work can be done to derive the power of the excitation sources in order to have more precise results. Also, even though the number of photons used in order to emit one higher energy photon is known, the number of total photons absorbed by the phosphor is not. If we knew the ratio of emitted UC photons to the total number of photons absorbed and emitted then the quantum efficiency and energy yield could be calculated. Another experiment to be conducted would be a direct solar energy test of the UC capabilities of the phosphor. Then, later the phosphors can be tested while applied to a solar cell. Not only could this test how well it can UC but to also analyze how much of an improvement is made to the solar cell.